Searches for displaced hadronic and lepton-jets at ATLAS

Edward Moyse

Introduction

- Many theories which predict existence of ‘long-lived’ particles.
- Will cover two **existing** ATLAS 8 TeV results
  - Long-lived, weakly interacting particles decaying to hadronic jets
    - Phys. Rev. D 92, 012010 (2015)
  - Pair produced, long-lived neutral particles decaying to hadronic jets
    - Physics Letters B 743 (2015) 15-34
- One **NEW** ATLAS 13 TeV result:
  - Search for long-lived neutral particles decaying into "lepton-jets" with the ATLAS detector in proton-proton collision data at sqrt(s) = 13 TeV
    - ATLAS-CONF-2016-042
    - See Antonio’s poster for more details:
      - 8 Aug 2016, 18:30, Riverwalk A/B

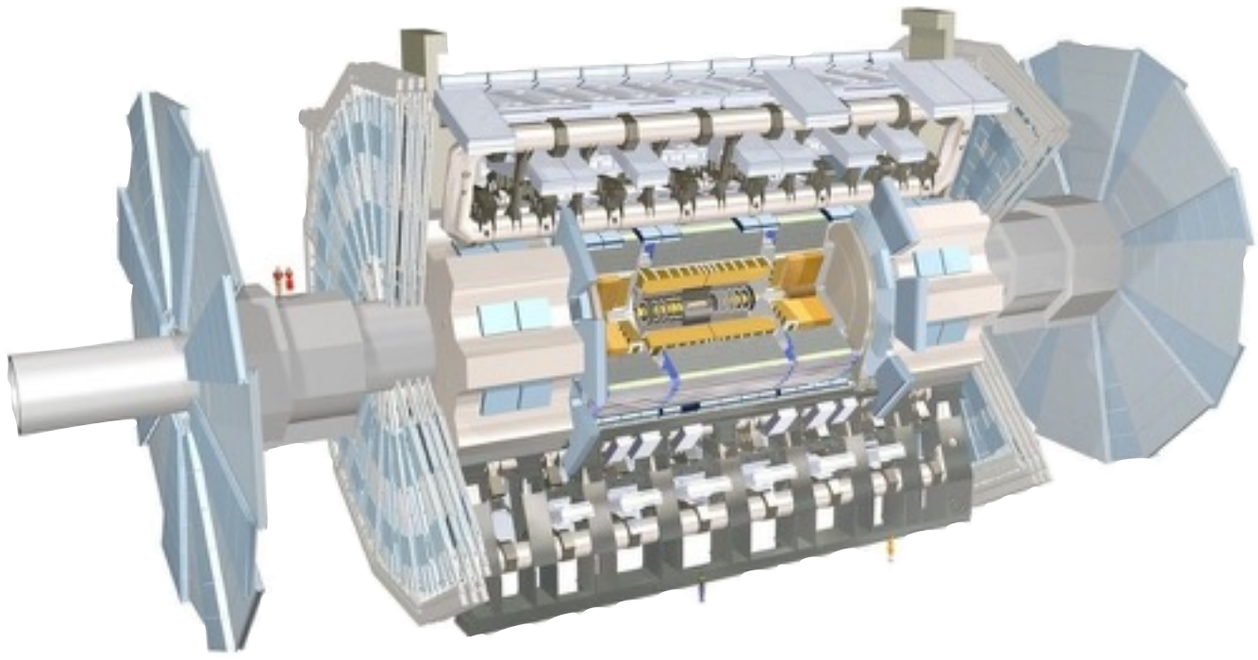

Hadronic jets

Physics models - hadronic jets

- ‘Hidden valley’ refers to a general class of models in which a hidden sector (v-sector) is added to SM
- v-particles don’t couple directly to SM, so need communicator particles:
  - Depending on coupling, this can lead to long lifetimes for the lightest v-particles
  - One benefit of having a large detector, is we have the ability to look for them!

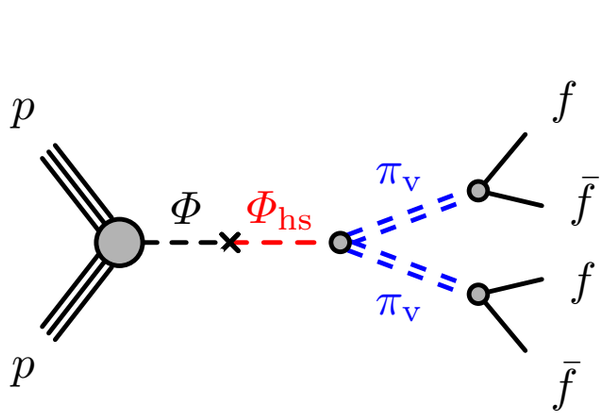

Scalar boson

Scalar-boson mixing with hidden-sector boson, Φ_{HS}.

Φ_{HS} decays to a pair of π_vs.

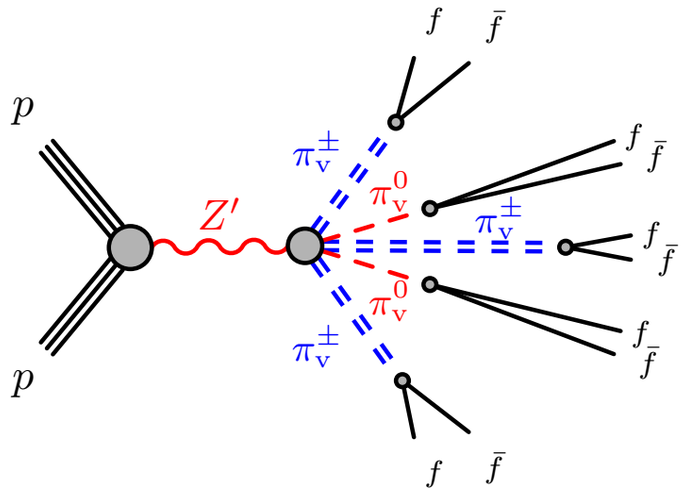

Z’

Z’ decays into v-quarks, which hadronize into π_vs.

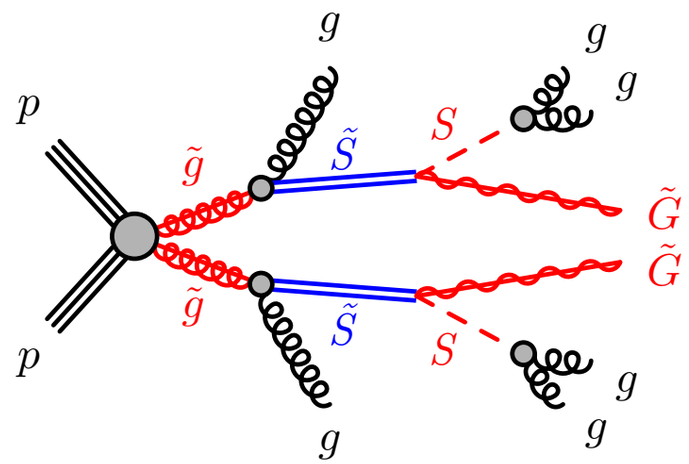

Stealth Susy

R-parity conserving SUSY models, which do not have large missing E_T.

This model: add a HS (stealth) singlet superfield S at the EW scale, which has super-partner singlino. Singlino decays to singlet and low mass gravitino

Reconstructing displaced jets

- **Triggering** - most standard triggers are linked to primary vertex, and are so very inefficient. Instead several specialised triggers are used by the various searches, including:
  - **Calo-Ratio trigger** : looks for >1 narrow jet with relatively little energy deposited in the EM calorimeter, and no charged tracks pointing towards to jet
  - **Muon-RoI-Cluster trigger** : looks for decays of neutral particles in the MS.

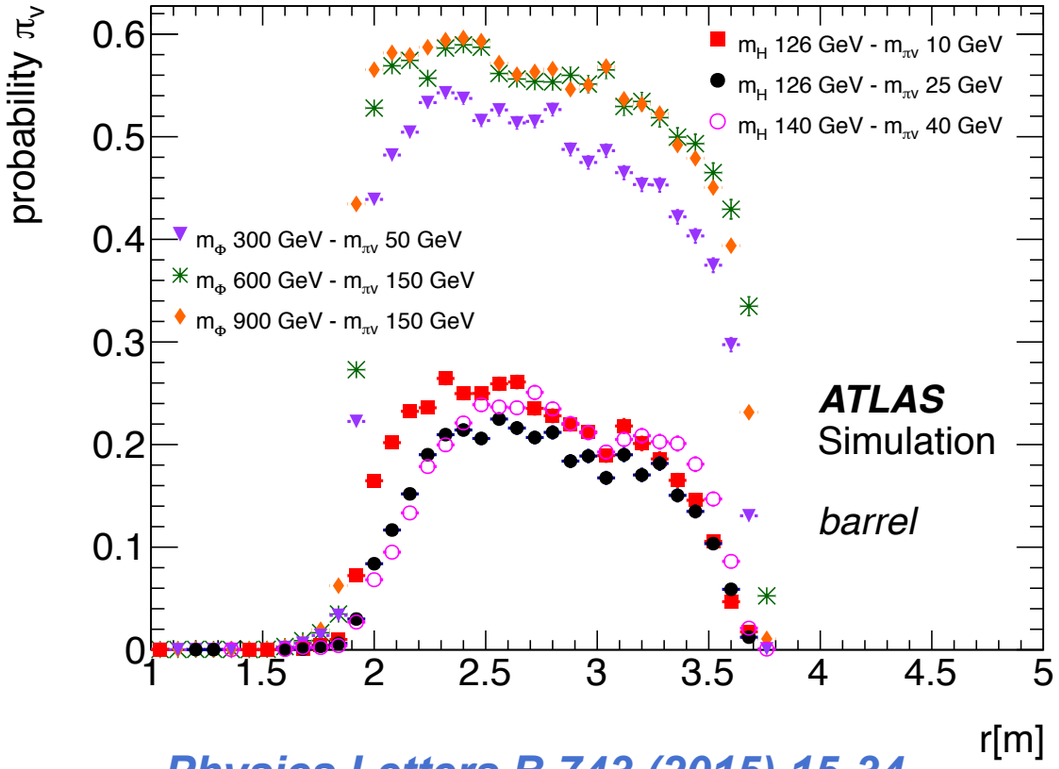

[Physics Letters B 743 (2015) 15-34]

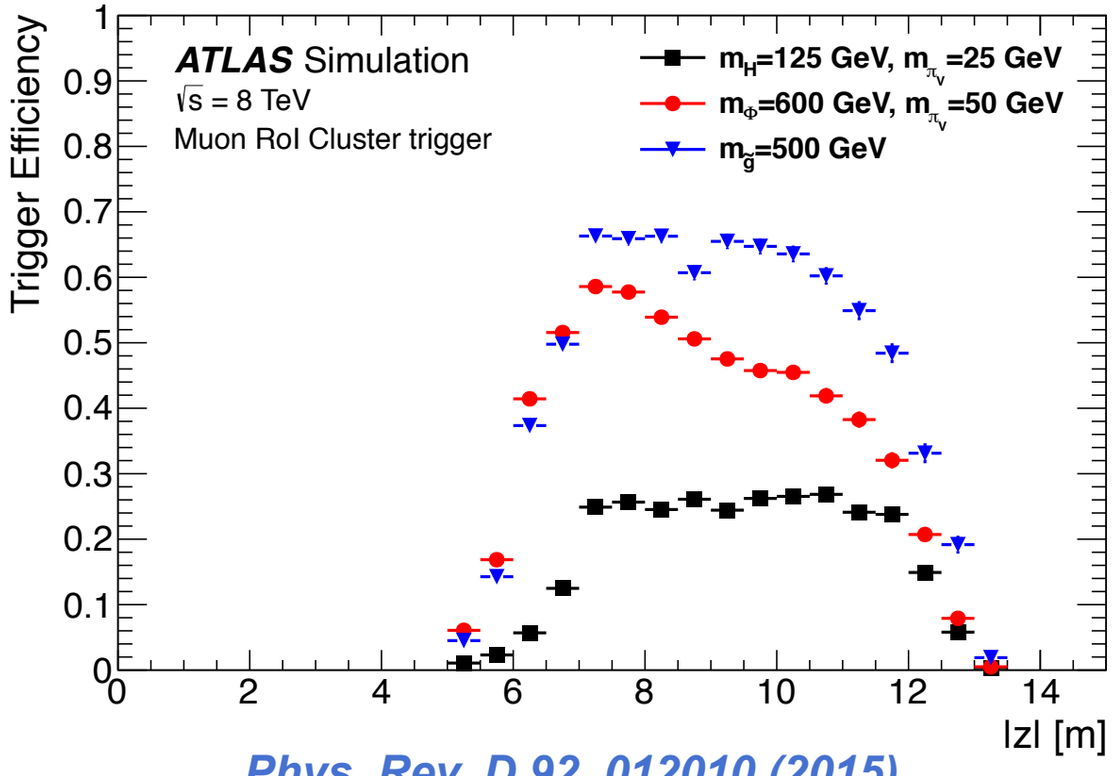

[Phys. Rev. D 92, 012010 (2015)]

Reconstructing muon vertices

- The spatial separation between the two multilayers inside a single MDT chamber provides a powerful tool for pattern recognition.
  - Generates ‘tracklets’ inside a single chamber.
- Specialised algorithm reconstructs straight line segments in multilayers, then matches segments using two parameters
  - Δb - minimum distance between segments at centre of chamber
  - Δα - angle between segments (can measure momenta for low pT muons)

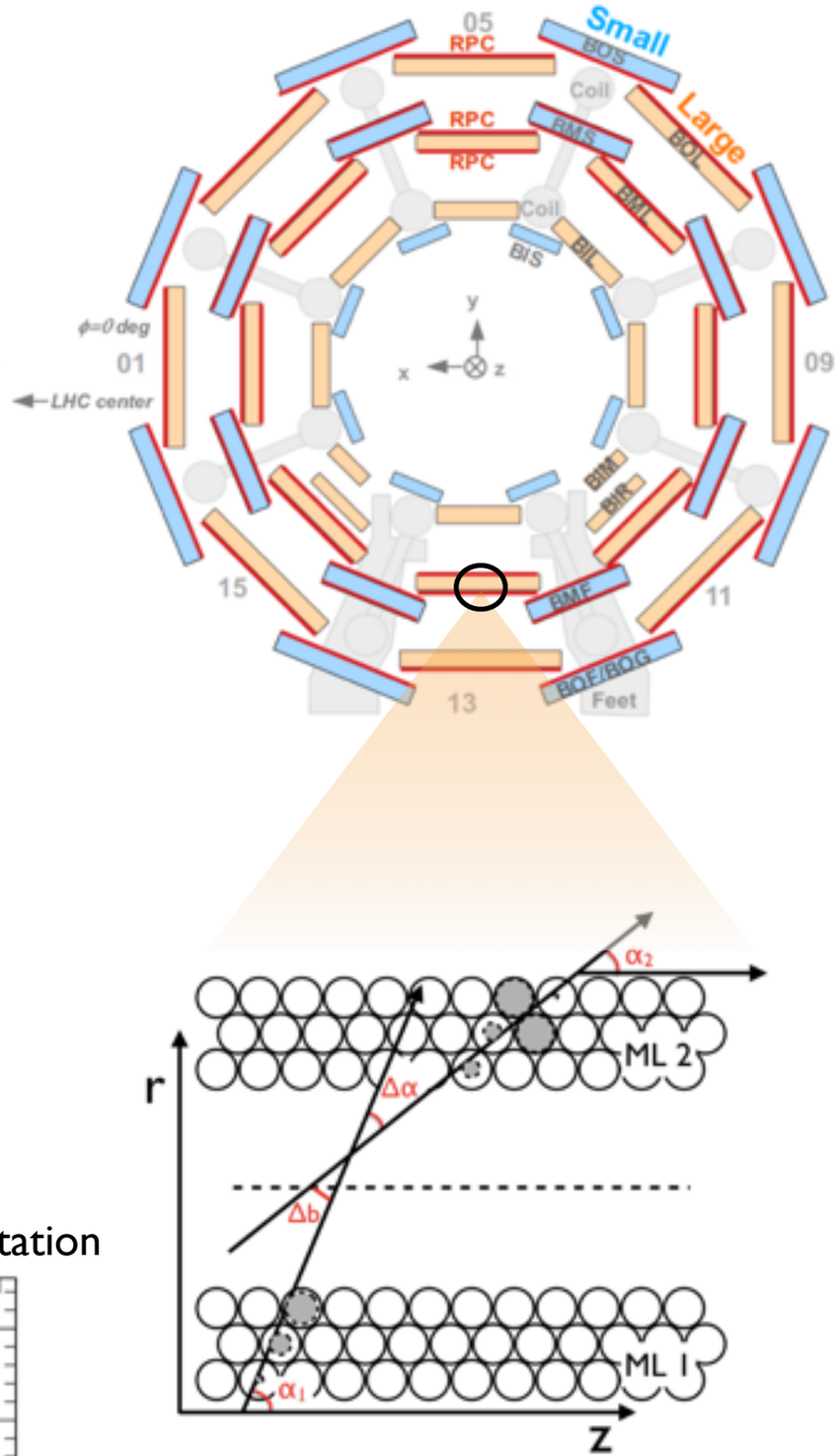

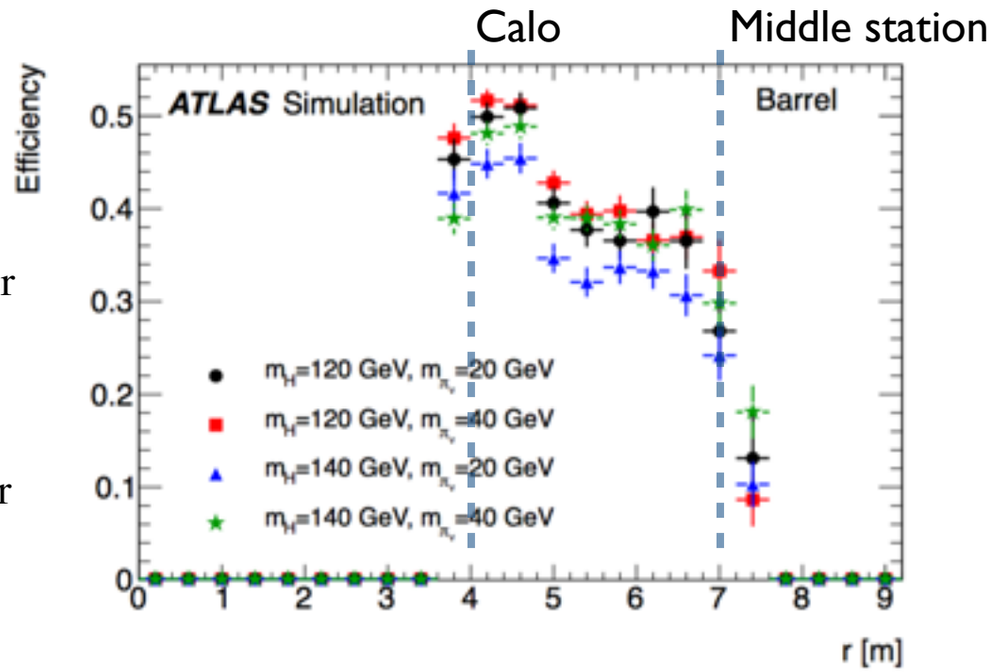

Efficiency for reconstructing a vertex for π_V decays in the barrel muon spectrometer as a function of the radial decay position of the π_V for π_V decays that satisfy the Muon RoI Cluster trigger

“Standalone vertex finding in the ATLAS muon spectrometer”

JINST 9, P02001 (2014), arXiv:1311.7070.

Results

Physics Letters B 743 (2015) 15-34

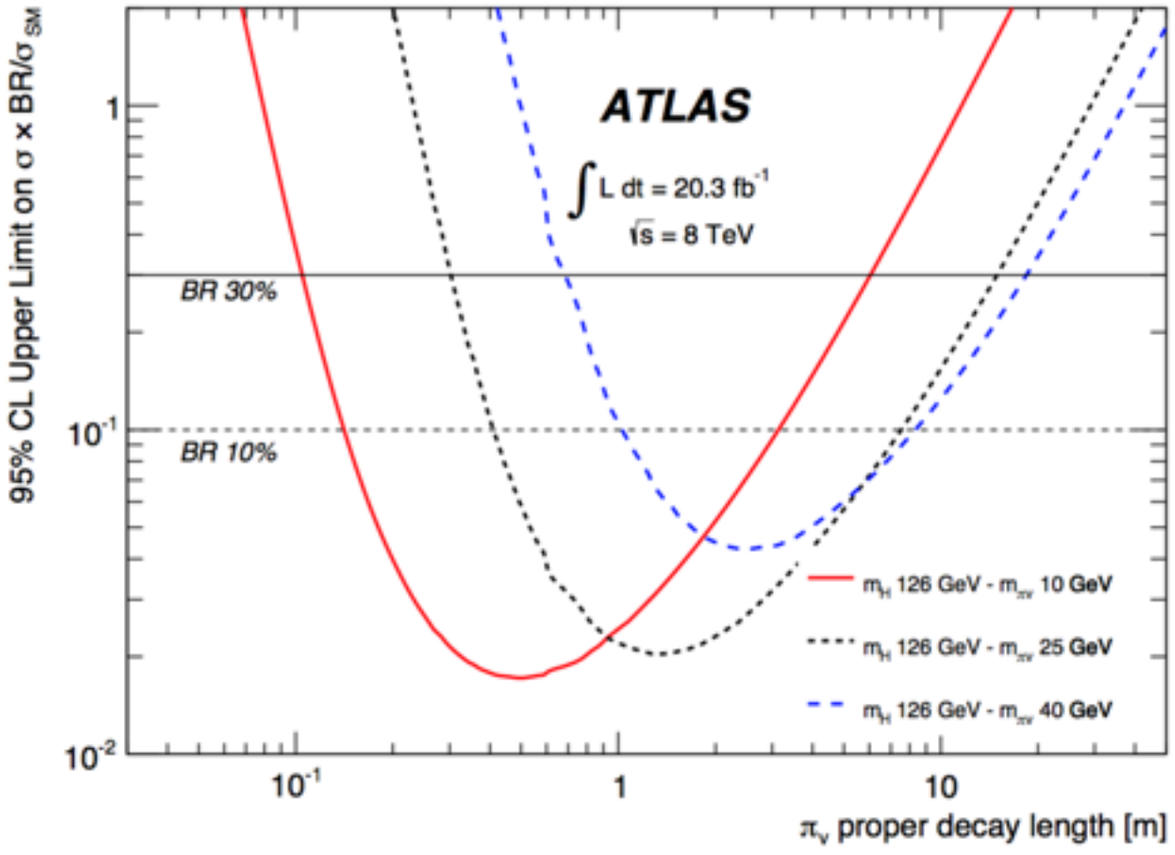

Observed 95% CL limits on σ /σSM for mH = 126 GeV as a function of the πv proper decay length: the solid line is for mπv = 10 GeV, the short-dashed line is for mπv = 25 GeV, the long-dashed line is for mπv = 40 GeV. The σSM is taken to be 19.0 pb. The horizontal solid line corresponds to BR = 30% and the horizontal dashed line to BR = 10%.

- No significant excess observed with 20.3 fb^{-1} of pp collisions

Sample (m_H, m_{π_v} [GeV])	Expected yields	Global acceptance (%)
126, 10	536 ± 23	0.139 ± 0.006
126, 25	941 ± 44	0.244 ± 0.011
126, 40	365 ± 31	0.095 ± 0.008

Background	Expected events
SM Multi-jets	23.2 ± 8.0
Cosmic rays	0.3 ± 0.2
Total Expected Background	23.5 ± 8.0
Data	24

- Limits set on π_v proper decay lengths for different π_v masses:

MC sample m_H, m_{π_v} [GeV]	Excluded range 30% BR $H \to \pi_v\pi_v$ [m]	Excluded range 10% BR $H \to \pi_v\pi_v$ [m]
126, 10	0.10 – 6.08	0.14 – 3.13
126, 25	0.30 – 14.99	0.41 – 7.57
126, 40	0.68 – 18.50	1.03 – 8.32

- (See paper for limits set for different Φ masses)

Results

Phys. Rev. D 92, 012010 (2015)

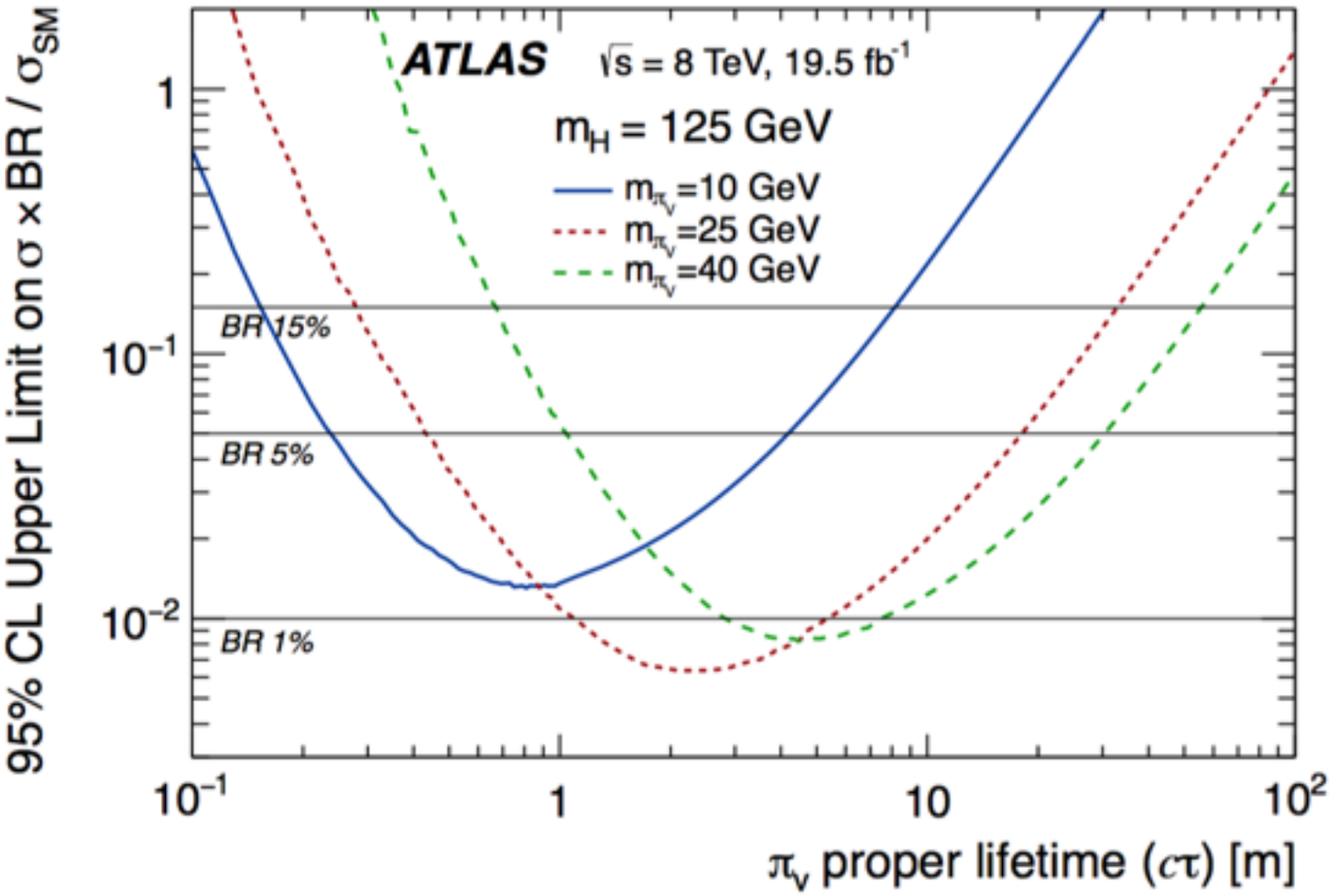

- No significant excess observed with 19.5 fb^{-1} (Muon RoI cluster trigger - see below) and 20.3 fb^{-1} (Jet + missing ET trigger)
- Limits set on π_v proper decay lengths

m_{π_v} [GeV]	Excluded $c\tau$ range [m]			
	1% BR	5% BR	15% BR	30 % BR
10	no limit	0.24–4.2	0.16–8.1	0.12–11.8
25	1.10–5.35	0.43–18.1	0.28–32.8	0.22–46.7
40	2.82–7.45	1.04–30.4	0.68–55.5	0.52–79.2

- (See paper for limits set for different Φ and gluino masses)

Topology	m_{π_v} [GeV]	Expected events		Observed events
		Signal	Background	
IDVx+MSVx	10	1.9 ± 1.4	2.0 ± 0.4	0
	25	62 ± 8		
	40	41 ± 6		
2 MSVx	10	234 ± 15	$0.4^{+0.3}_{-0.2}$	2
	25	690 ± 26		
	40	313 ± 18		

Expected signal for scalar boson model
m_H=125 GeV and $c\tau$=2m


UNIVERSITY OF MASSACHUSETTS
AMHERST 1863
ENSE PETIT PLACIDAM SUB LIBERTATE QUIETEM

Lepton-jets

Physics models - Lepton-jets

- Signature models are Falkowsky-Ruderman-Volansky-Zupan (FRVZ) where Higgs boson decays to pairs of hidden fermions:

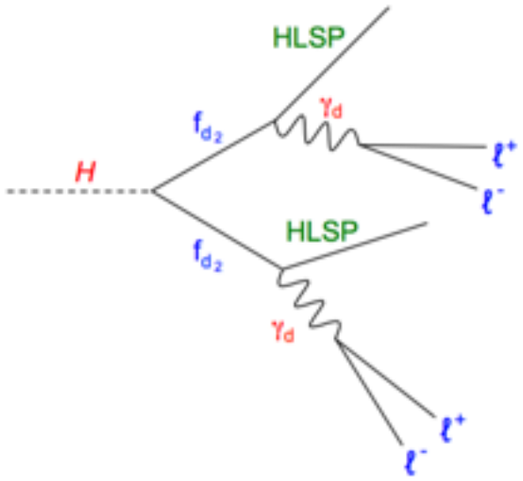

In the first benchmark model, the dark fermion decays to a γ_d and a lighter dark fermion f_{d_1}, HLSP (Hidden Lightest Stable Particle).

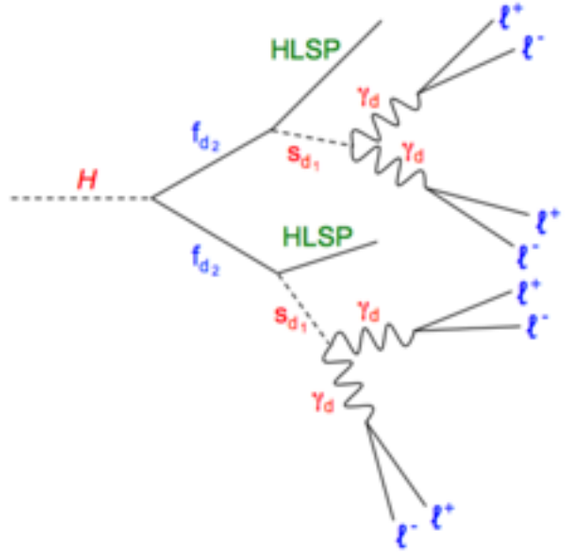

In the second model, the dark fermion f_{d_2} decays to an HLSP and a dark scalar s_{d_1} that in turn decays to pairs of dark photons.

- Photons typically produced with large boost
  - collimated jet-like structures containing pairs of muons/electrons and/or pions
    - "lepton-jets"
  - Limited granularity of detectors makes resolving constituents challenging…

NEW

Lepton-jets

- Search for long-lived neutral particles decaying into displaced lepton-jets in proton--proton collisions at $\sqrt{s}$ = 13 TeV with the ATLAS detector (2015 data)
  - ATLAS-CONF-2016-042
- Integrated luminosity for search is 3.57 fb^{-1}
  - However despite lower integrated luminosity, sensitivity is comparable to 2012 dataset at 8 TeV, due to:
    - Improvements in trigger sensitivity and reconstruction efficiency for close-by muons
    - Higher cross section for Higgs production at 13 TeV

NEW

Lepton jet reconstruction

- At detector level, LJs categorised according to content:

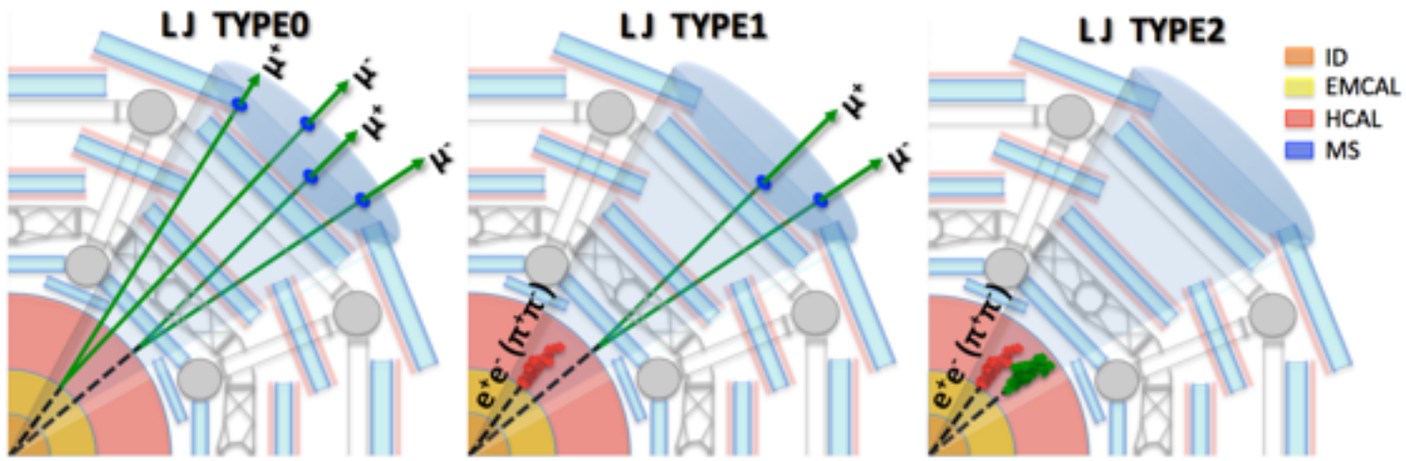

- Muonic LJs reconstructed by ‘clustering’ all muon tracks within the cone, seeded from highest-p_T muon track.

- Acceptance * Efficiency vs transverse decay distance:

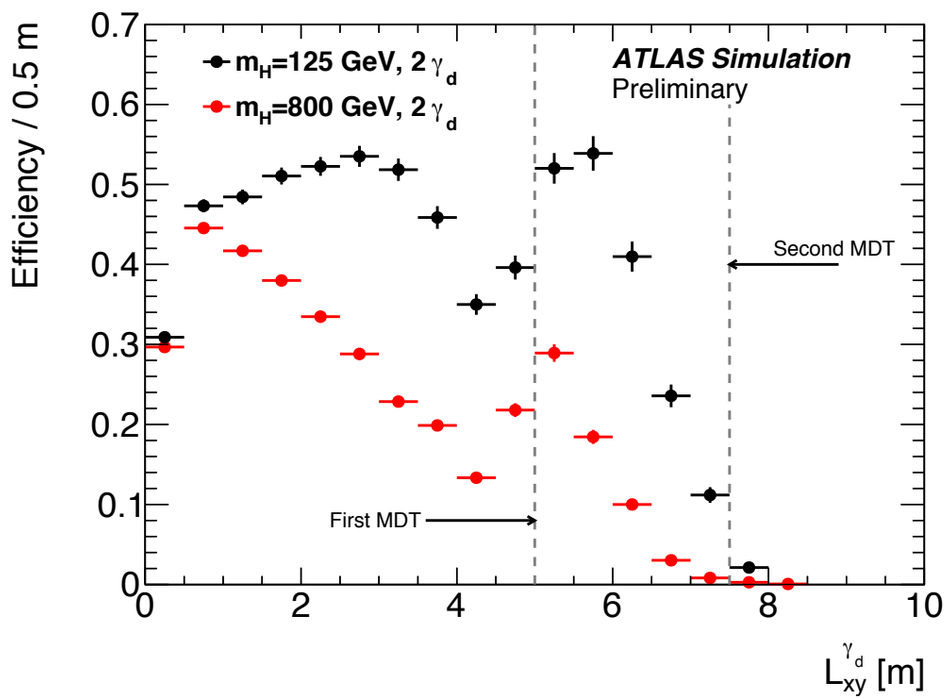

NEW

Results - Lepton-jets

- No excess -> so set limits (excluding Type2-Type2 channel, which has low efficiency and high background):

Category	Observed events	Expected background
All events	285	231 ± 12 (stat) ± 62 (syst)
Type2–Type2 excluded	46	31.8 ± 3.8 (stat) ± 8.6 (syst)
Type2–Type2 only	239	241 ± 41(stat) ± 65(syst)

FRVZ model	m_{H} (GeV)	Excluded cτ [mm]
Higgs $\rightarrow 2\gamma_{\mathrm{d}} + X$	125	$2.2 \leq c\tau \leq 111.3$
Higgs $\rightarrow 4\gamma_{\mathrm{d}} + X$	800	$3.8 \leq c\tau \leq 163.0$
Higgs $\rightarrow 2\gamma_{\mathrm{d}} + X$	125	$0.6 \leq c\tau \leq 63$
Higgs $\rightarrow 4\gamma_{\mathrm{d}} + X$	800	$0.8 \leq c\tau \leq 186$

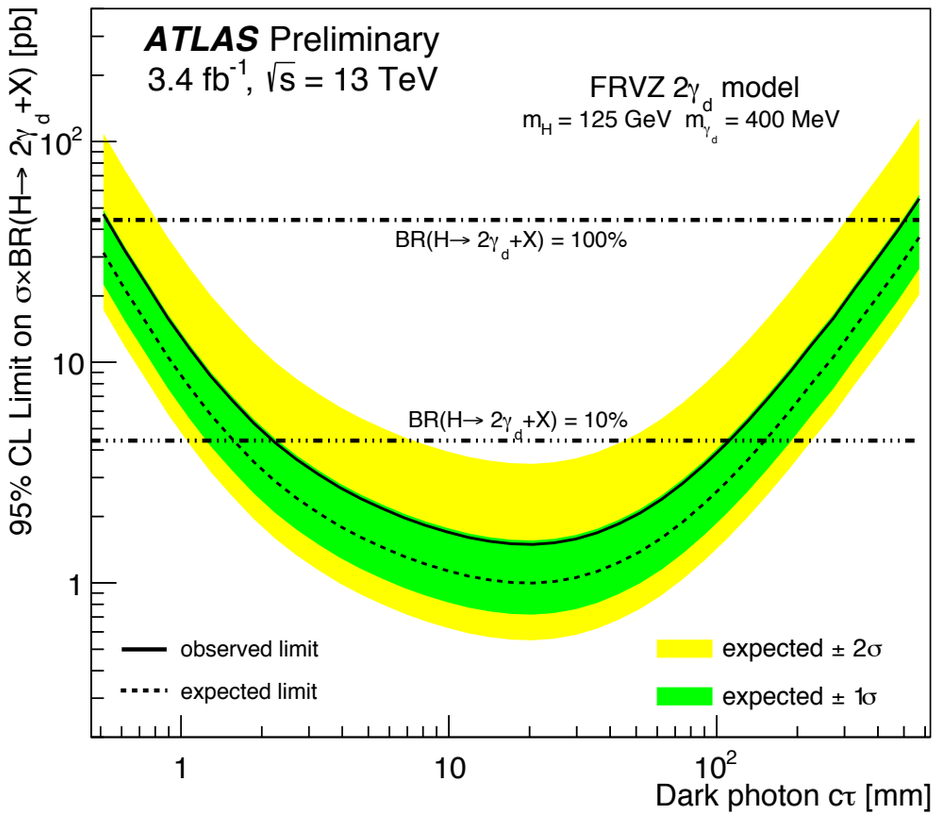

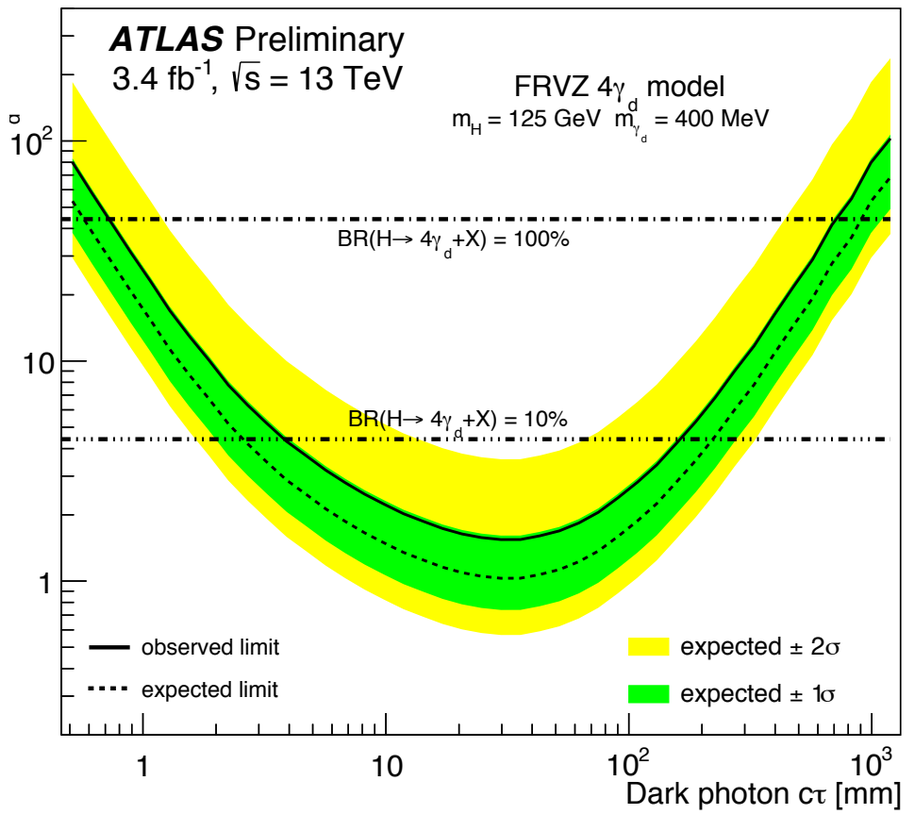

Conclusion

- Presented two 8 TeV analyses for long-lived particles decaying to hadronic jets
  - *Phys. Rev. D 92, 012010 (2015)* and *Physics Letters B 743 (2015) 15-34*

- Presented 13 TeV results for Displaced lepton-jets
  - ATLAS-CONF-2016-042

- Thank you very much for your time and attention.

Backup

- Pair produced, long-lived neutral particles decaying to hadronic jets
  - Physics Letters B 743 (2015) 15-34
  - “Calo-ratio”

Calo ratio - data and samples

- **Data**: 20.3 fb-1 taken in 2012
- **MC**

The HV Monte Carlo (MC) samples are generated with PYTHIA 8.165 [16] and the PDF MSTW2008 [17] to simulate gluon fusion $gg \rightarrow \Phi$ production and the Φ_{hs} decay $\Phi_{hs} \rightarrow \pi_V \pi_V$ for different Φ and π_V masses (Table 1). Φ masses below 300 GeV are consid- ered low-mass samples and the rest are considered high-mass samples. The π_V lifetime is fixed in each sample to ensure decays throughout the ATLAS detector. The Φ is simulated in PYTHIA by replacing the Higgs boson with the Φ and having the Φ decay to π_V 100% of the time.

Table 1: The Φ mass or Higgs boson mass, Φ gluon fusion production cross section, and π_v mass of each benchmark Hidden Valley model generated. The cross-sections are based on the assumption in the benchmarked model that the Φ boson production mechanism is the same as the Higgs boson production mechanism. The decay branching ratios of the π_v as a function of the π_v mass are listed in the second table as determined in the simulation samples.

m_H [GeV]	σ [pb]	π_v Mass [GeV]
126	19.0	10, 25, 40

Φ Mass [GeV]	σ [pb]	π_v Mass [GeV]
100	29.7	10, 25
140	15.4	10, 20, 40
300	3.59	50
600	0.52	50, 150
900	0.06	50, 150

π_v Mass [GeV]	BR $b\bar{b}$ [%]	BR $\tau^+\tau^-$ [%]	BR $c\bar{c}$ [%]
10	70.0	16.4	13.4
20	86.3	8.0	5.6
25	86.6	8.1	5.3
40	86.5	8.5	5.0
50	86.2	8.8	4.9
150	84.8	10.2	4.8

Calo ratio - trigger

- looks for >1 narrow jet with relatively little energy deposited in the EM calorimeter, and no charged tracks pointing towards to jet

The trigger is tuned to look for events containing at least one narrow jet with little energy deposited in the ECal and no charged tracks pointing towards the jet.

At the first level the trigger selects only narrow jets by requiring at least 40 GeV of transverse energy (E_T) in the calorimeter in a 0.2×0.2 ($\Delta\eta \times \Delta\phi$) region using topological jets [15, 22], in contrast to the default algorithm in which the energy in a 0.4×0.4 region is summed.

The 40 GeV E_T threshold requirement is fully efficient at an offline jet E_T of 60 GeV. To select jets with a high fraction of their energy in the HCal the second level of the trigger requires these narrow jets to have $\log_{10}(E_H/E_{EM}) > 1.2$, where E_H/E_{EM} is the ratio of the energy deposited in the HCal (E_H) to the energy deposited in the ECal (E_{EM}). The trigger also requires no tracks with $p_T > 1$ GeV in the region 0.2×0.2 ($\Delta\eta \times \Delta\phi$) around the jet axis. The third

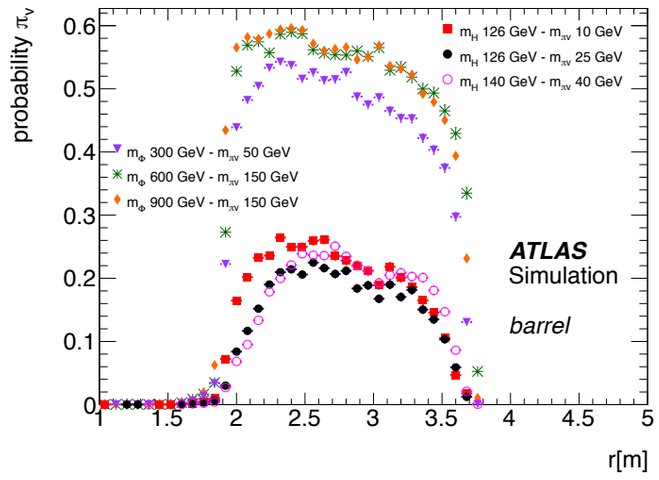

(a)

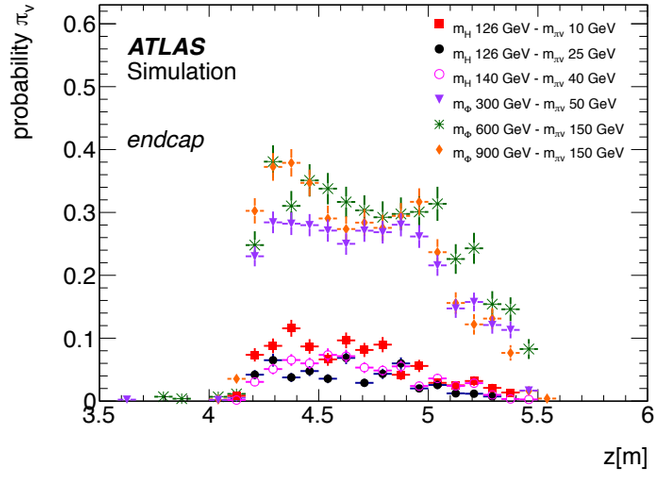

(b)

Fig. 1: The probability (ε_{π_v}) for a single π_v to pass the trigger as a function of the π_v (a) radial decay length in the barrel and (b) the z position of the decay vertex in the endcaps for several Φ and π_v masses.

Calo ratio - backgrounds

- The largest contribution to the expected background comes from SM multi-jet events.
  - Cosmics rays much less, and beam halo negligible
- To estimate the multi-jet background contribution, a multi- jet data sample is used to derive the probability that a jet passes the trigger and analysis selection
- The multi-jet data sample contains events that pass single-jet triggers with an ET threshold of 15 GeV or higher.
  - Require >2 back to back jets
    - 1 jet must pass the modified ATLAS good-jet criteria used by the analysis.
    - 2nd used to measure two probabilities:
      - P, for a jet to pass the trigger and the ET > 60 GeV jet requirement
      - Q, for a jet to satisfy the requirement ET > 40 GeV.
    - For both P and Q the jet must also pass the log10(EH/EEM), track isolation, and all other analysis jet selection requirements including the modified ATLAS good-jet criteria.

Calo ratio - backgrounds (2)

- Cosmic ray:
  - Particles from a cosmic-ray shower may pass through and deposit energy in the calorimeter without passing through the ID. These energy deposits can be reconstructed as trackless jets.
  - Reduce with jet-timing and Etmiss requirements
  - Study with empty BC
- BIB
  - beam-halo muon that undergoes bremsstrahlung in the HCal.
  - A jet-timing requirement is imposed because most of the jets pro- duced by beam-halo interactions are not coincident in time with jets from pp interactions. In addition, events are rejected when track segments in the endcap muon chambers, from the entering beam-halo muon, align in ϕ with a jet. These two requirements reduce the background considerably with no discernible effect on the signal

Calo ratio - systematic uncertainties

- The uncertainty on the signal MC samples due to parton distribution functions (PDF) is calculated by reweighting each event using three different PDF sets (MSTW2008nlo68cl [17], CT10 [27], and NNPDF2.3 [28]) and their associated error sets. The RMS change in acceptance for the error sets of each PDF is calculated and combined with the difference in acceptances for each of the three PDFs.
- Pile-up primarily affects the acceptance by adding extra tracks and degrading the track isolation of a jet. All MC samples are reweighted to reproduce the observed distribution of the number of interactions per bunch crossing in the data. To determine if pile-up is simulated properly in the MC samples, a direct comparison of data and MC multi-jet samples is per-formed. The jet ET, EMF, η, ϕ, associated tracks and timing distributions as a function of the mean number of pile-up in- teractions are compared in data and MC simulation. A 10% systematic uncertainty is assigned to the acceptance covers all the observed differences.

Table 2: Summary of systematic uncertainties for the Φ and Higgs boson production cross-section, jet energy scale, trigger, missing transverse momentum, and the requirement on jet timing as a percentage of the signal yield. Systematic errors that have common values across samples are not listed (pile-up at 10%, ISR at $^{+2.9}_{-1.2}$%, and PDF at 2.1%). The last column reports the total systematic uncertainty (including the luminosity and common systematic errors).

Sample m_H, m_{π_v} [GeV]	H σ [%]	JES [%]	Trigger [%]	E_T^{miss} [%]	Time Cut [%]	Total [%]
126, 10	$^{+10.4}_{-10.4}$	$^{+2.2}_{-2.7}$	±1.1	$^{+5.5}_{-2.4}$	$^{+1.6}_{-6.6}$	$^{+16.4}_{-16.7}$
126, 25	$^{+10.4}_{-10.4}$	$^{+1.5}_{-1.6}$	±1.3	$^{+3.1}_{-1.8}$	$^{+0.8}_{-3.3}$	$^{+15.6}_{-15.5}$
126, 40	$^{+10.4}_{-10.4}$	$^{+2.6}_{-6.2}$	±1.1	$^{+7.7}_{-4.6}$	$^{+1.9}_{-5.9}$	$^{+18.2}_{-16.9}$
Sample m_Φ, m_{π_v} [GeV]	Φ σ [%]	JES [%]	Trigger [%]	E_T^{miss} [%]	Time Cut [%]	Total [%]
100, 10	$^{+11.1}_{-10.6}$	$^{+2.3}_{-4.0}$	±0.1	$^{+4.6}_{-3.4}$	$^{+2.7}_{-9.5}$	$^{+16.7}_{-18.5}$
100, 25	$^{+11.1}_{-10.6}$	$^{+5.5}_{-3.7}$	±1.2	$^{+3.4}_{-2.5}$	$^{+1.7}_{-0.7}$	$^{+17.0}_{-15.8}$
140, 10	$^{+10.1}_{-10.3}$	$^{+0.6}_{-1.1}$	±0.5	$^{+4.0}_{-5.6}$	$^{+1.9}_{-6.6}$	$^{+15.6}_{-17.2}$
140, 20	$^{+10.1}_{-10.3}$	$^{+1.2}_{-1.6}$	±1.0	$^{+4.0}_{-3.9}$	$^{+0.4}_{-5.0}$	$^{+15.5}_{-16.2}$
140, 40	$^{+10.1}_{-10.3}$	$^{+1.3}_{-1.6}$	±1.5	$^{+6.3}_{-4.6}$	$^{+1.8}_{-2.4}$	$^{+16.5}_{-15.8}$
300, 50	$^{+9.6}_{-10.0}$	$^{+0.1}_{-0.3}$	±0.3	$^{+9.0}_{-7.4}$	$^{+0.5}_{-3.0}$	$^{+13.9}_{-13.3}$
600, 50	$^{+11.2}_{-10.1}$	$^{+0.0}_{-0.1}$	±0.2	$^{+11.7}_{-11.3}$	$^{+2.2}_{-4.4}$	$^{+17.0}_{-16.2}$
600, 150	$^{+11.2}_{-10.1}$	$^{+0.2}_{-0.2}$	±0.3	$^{+11.5}_{-10.2}$	$^{+2.7}_{-5.3}$	$^{+17.5}_{-15.1}$
900, 50	$^{+12.8}_{-11.5}$	$^{+0.0}_{-0.1}$	±0.1	$^{+12.6}_{-9.7}$	$^{+1.0}_{-3.7}$	$^{+18.5}_{-15.9}$
900, 150	$^{+12.8}_{-11.5}$	$^{+0.2}_{-0.3}$	±0.2	$^{+11.8}_{-10.9}$	$^{+0.9}_{-2.5}$	$^{+18.1}_{-16.3}$

Calo - results and limits

- CLs method used to derive an upper limit on the σ(Φ)×BR(Φ → πνπν).
- A profile likelihood ratio is used as the test statistic and a frequentest calculator is used to generate toy data.
- The likelihood includes a Poisson probability term describing the total number of observed events. Systematic uncertainties are incorporated as nuisance parameters through their effect on the mean of the Poisson functions and through convolution with their assumed Gaussian distributions. The number of expected events in signal MC samples, together with the estimate of expected background, the observed collision events and all the systematic uncertainties are provided as input for computing the CLs value, which represents the probability for the given observation to be compatible with the signal + background hypothesis.

Sample (m_H, m_{π_v} [GeV])	Expected yields	Global acceptance (%)
126, 10	536 ± 23	0.139 ± 0.006
126, 25	941 ± 44	0.244 ± 0.011
126, 40	365 ± 31	0.095 ± 0.008

Sample (m_H, m_{π_v} [GeV])	Expected yields	Global acceptance (%)
100, 10	440 ± 29	0.073 ± 0.005
100, 25	424 ± 37	0.070 ± 0.006
140, 10	525 ± 20	0.168 ± 0.006
140, 20	900 ± 37	0.287 ± 0.012
140, 40	641 ± 30	0.205 ± 0.010
300, 50	444 ± 11	0.609 ± 0.015
600, 50	35 ± 1	0.330 ± 0.010
600, 150	41 ± 2	0.386 ± 0.015
900, 50	3.5 ± 0.1	0.304 ± 0.011
900, 150	4.6 ± 0.2	0.397 ± 0.016

Background	Expected events
SM Multi-jets	23.2 ± 8.0
Cosmic rays	0.3 ± 0.2
Total Expected Background	23.5 ± 8.0
Data	24

Vertex - intro

Search for long-lived, weakly interacting particles that decay to displaced hadronic jets in proton–proton collisions at $\sqrt{s} = 8$ TeV with the ATLAS detector

- Long-lived, weakly interacting particles decaying to hadronic jets
  - Phys. Rev. D 92, 012010 (2015)
  - “MS/ID vertexing”

Vertex - analysis strat

- Hadronic decays that are displaced from the IP leave a unique detector signature that can be reconstructed as a displaced vertex. This analysis searches for events with two displaced vertices in either the ID or MS, or one in each.
- This analysis studies two separate channels, defined by the triggers used to select events.
  - ATLAS Muon RoI Cluster trigger is used to preselect events that satisfy displaced-decay criteria in the MS. The search for both the scalar boson and Stealth SUSY models makes use of events selected by the Muon RoI Cluster trigger. The sample of events selected by this trigger belongs to the Muon Cluster channel.
  - A jet plus E miss trigger : The large multiplicity of long-lived particles in the Z′benchmark samples causes many events to fail to satisfy the isolation criteria of the Muon RoI Cluster trigger, but also provides other objects on which to trigger.
- To reduce backgrounds, two vertices req.

TABLE I. The topologies considered in the analysis and the corresponding triggers and benchmark models.

Trigger	Applicable topologies	Benchmarks
Muon RoI Cluster	IDVx+MSVx, 2MSVx	Scalar boson, Stealth SUSY
Jet+$E_{\mathrm{T}}^{\mathrm{miss}}$	2IDVx, IDVx+MSVx, 2MSVx	Z'

Data / MC

The dataset used in this analysis was recorded by the ATLAS detector in the 2012 run during periods in which all subdetectors relevant to the analysis were operating efficiently. The integrated luminosity is 20.3 fb^{-1}. The Muon Cluster channel uses only 19.5 fb^{-1} of data because the trigger was not active at the beginning of the run. The uncertainty on the integrated luminosity, estimated following the methodology described in Ref. [31], is 2.8%.

TABLE II. Mass parameters for the simulated scalar boson, $Z'$and Stealth SUSY models.

Scalar boson mass [GeV]	π_v mass [GeV]
100	10, 25
125	10, 25, 40
140	10, 20, 40
300	50
600	50, 150
900	50, 150
Z'mass [TeV]	π_v mass [GeV]
1	50
2	50
2	120
$\tilde{g}$ mass [GeV]	$\tilde{S}$, S mass [GeV]
110	100, 90
250	100, 90
500	100, 90
800	100, 90
1200	100, 90

Vertex - Muon ROI cluster trigger

The Muon RoI Cluster trigger is a signature-driven trigger that selects decays of neutral particles in the MS. It is used to select candidate events for the scalar boson and Stealth SUSY searches, and is efficient for hadronic decays occurring in the region from the outer radius of the HCal to the middle of the MS. The trigger selects events with a cluster of muon RoIs contained in a $\Delta R = 0.4$ cone that are preceded by little or no activity in the ID or calorimeters. This isolation requirement reduces backgrounds from muon bremsstrahlung and punch-through jets. A punch-through jet is a hadronic or electromagnetic shower not contained in the calorimeter volume, which results in tracks in the MS. The details of the performance and implementation of this trigger on both a set of MC simulated benchmark samples and data can be found in Ref. [27].

B. Jet+$E_{\mathrm{T}}^{\mathrm{miss}}$trigger

A single-jet plus $E_{\mathrm{T}}^{\mathrm{miss}}$trigger is employed for the Z'search. The trigger uses a leading jet E_{T}threshold of 110 GeV and an $E_{\mathrm{T}}^{\mathrm{miss}}$threshold of 75 GeV. Offline requirements are a leading jet $p_{\mathrm{T}} \geq 120$ GeVand $E_{\mathrm{T}}^{\mathrm{miss}} \geq 200$ GeV, which result in a constant trigger efficiency as a function of both p_{T} and $E_{\mathrm{T}}^{\mathrm{miss}}$. For events passing the offline requirements, the trigger efficiency is 87–100%, depending on the MC simulated Z'benchmark sample.

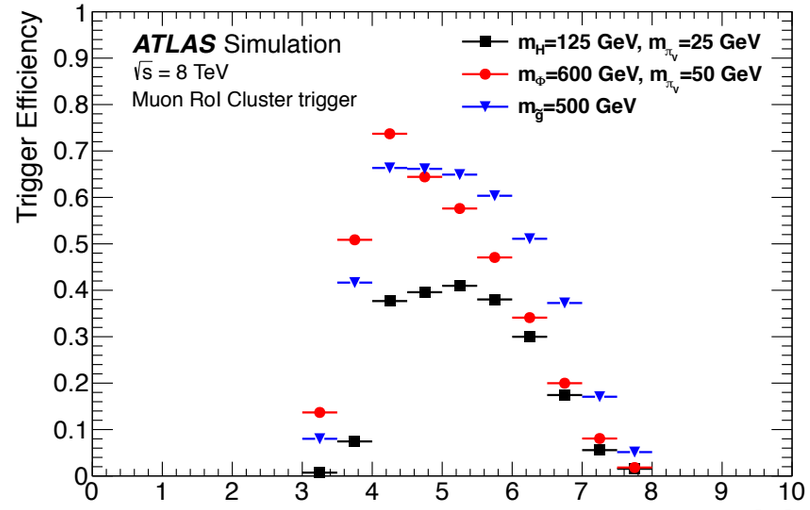

FIG. 2. Efficiency for the Muon RoI Cluster trigger in the barrel as a function of the decay position of the long-lived particle for three simulated benchmark samples.

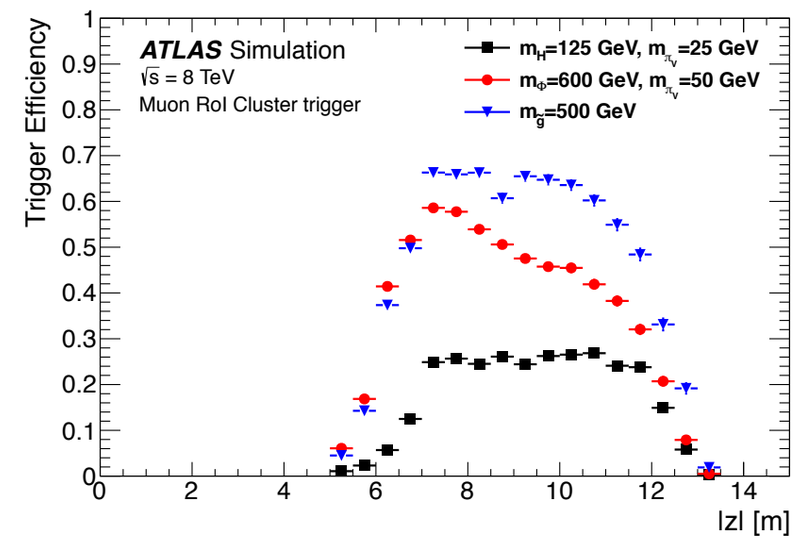

FIG. 3. Efficiency for the Muon RoI Cluster trigger in the endcaps as a function of the the decay position of the long-lived particle for three simulated benchmark samples.

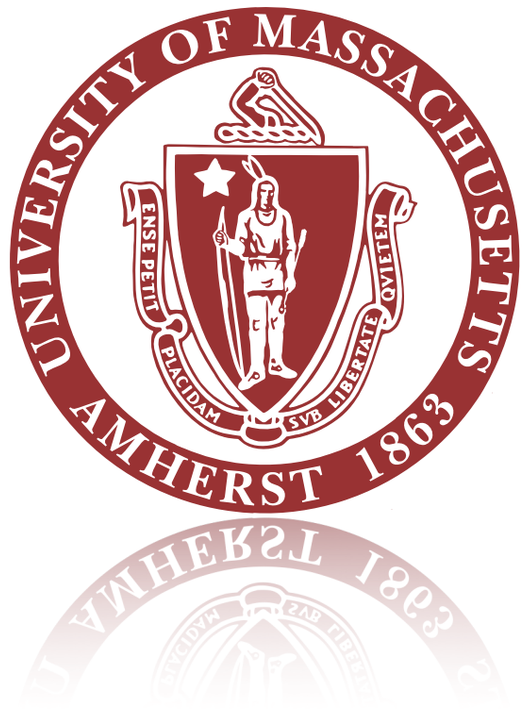
UNIVERSITY OF MASSACHUSETTS
AMHERST 1863
ENSE PETIT PLACIDAM SVB LIBERTATE QVIETEM

Lepton jets

LJ - triggers

- **Narrow-Scan**: The Narrow-Scan trigger was introduced for the 2015 data-taking, and adopts a specialised and novel approach for a wide range of signal models featuring highly collimated muons such as in the LJ case. The Narrow-Scan algorithm begins with requiring at least one L1 trigger muon object. Other multi-muon triggers, which usually require more L1 trigger muon objects, have large associated signal efficiency losses in the case where the muons are produced close together.

- **Tri-muon** MS-only [51]: selects events with at least three MS-only muons with pT ≥ 6 GeV. It is seeded at L1 by a cluster of three muon ROIs in a ΔR = 0.4 cone, and is required to have no reconstructed jets within a cone of ΔR = 0.5.

- **CalRatio** [51]: selects events with an isolated jet of low EM fraction. The CalRatio trigger is seeded by a L1 tau-lepton trigger with pT ≥ 60 GeV. A L1 tau-lepton seed was chosen over a jet seed because the L1 τ seed uses a narrower calorimeter region than the L1 jet seed. Decays of γd in the HCAL tend to produce narrow jets. The trigger requires the jet to have |η| ≤ 2.4 (to ensure that ID tracks can be matched to it) and ET ≥ 30 GeV. A selection requirement on the calorimeter energy ratio is then imposed, requiring log(EHCAL/EECAL) ≥ 1.2. Finally, ID track isolation selection around the jet axis (no track with pT ≥ 2 GeV within ΔR ≤ 0.2 from the jet axis) and BIB tagging are performed to reject fake jets from beam-halo muons.

LJ - backgrounds

- Cosmic-ray muons that cross the detector in time coincidence with a pp interaction constitute the main source of background to the Type0 signal, and a sub-dominant background to the Type1 and Type2 signals.

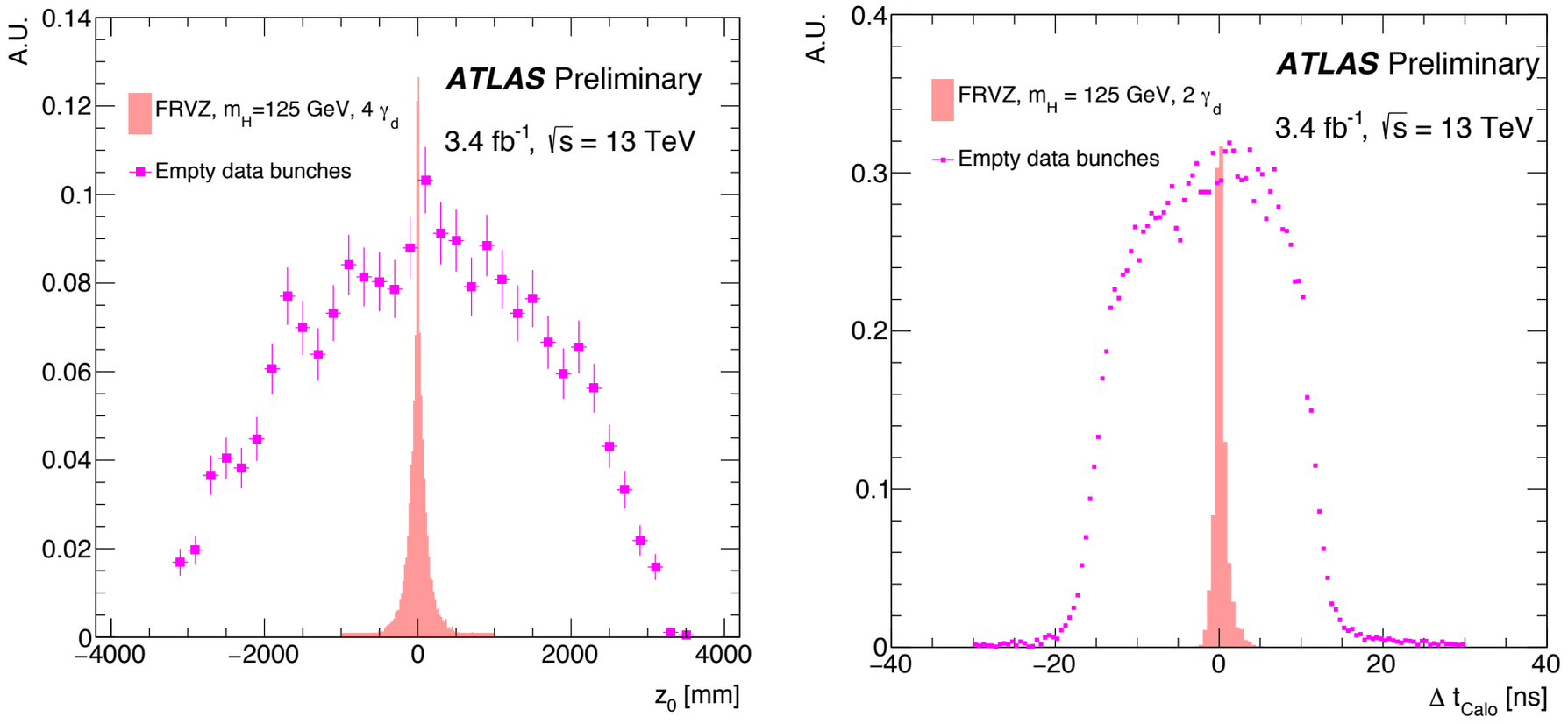

Figure 3: The muon impact parameter $|z_0|$ (left) for muonic LJ constituents in empty bunch-crossings (cosmic-ray muons) and for muonic LJ constituents in the $m_H = 125$ GeV FRVZ Higgs $\rightarrow 4\gamma_d + X$ case. The jet timing, Δt_{Calo}, (right) of Type2 LJs from signal MC and single jet triggered events in empty bunch-crossings. In both plots, data refers to the 2015 data taking.

Removing jets with Δt_{Calo} outside the interval between −4 ns and +4 ns removes a large fraction of the cosmic-ray jets, with a loss of signal less than 5%.

A selection requirement |z0| ≤ 280 mm is used; in this way only 5% of the signal in the Higgs → 4γd + X sample is lost while eliminating 96% of the cosmic-ray background

LJ - backgrounds (2)

- Multijet production constitutes the main background to the Type2 LJ signal. The search explicitly targets γd decays in the HCAL, resulting in most of the energy deposition occurring in the HCAL rather than in the ECAL. Therefore, low EM fraction is an effective criterion to distinguish jets in Type1 and Type2 LJs from multijet background.
- Another effective discriminating variable is the jet width W, defined as the average distance of a jet constituent to the jet direction weighted with the energy of the constituent
- Beam-induced background (BIB), consisting of high energy beam-halo muons undergoing hard bremsstrahlung in the calorimeters, is another sub-dominant source of background for Type2 LJs. The bremsstrahlung manifests itself as a calorimeter deposit that is reconstructed as a jet; if it occurs in the HCAL, the fake jet is reconstructed with a very low EM fraction. BIB “tagging” searches for two track segments parallel to the beam line in the forward MDT chambers, together with a low EM fraction HCAL jet, all within 4 degrees in ϕ. Such an HCAL jet is tagged as BIB and removed from the data set.

5.7 Summary of preselection requirements

A summary of the LJ signal selection requirements is given in Table 3.

LJ type	Selection requirement	Requirement description
Type 0/1	z_0 limits	an impact parameter $\lvert z_0 \rvert < 280$ mm for both muons of the LJ
Type 1/2	jet timing Δt_{Calo}	remove jets outside the ± 4 ns time window
Type2	tile-gap scint.	max energy in tile-gap scintillators ≤ 10% of the jet energy
Type2	EM fraction	EM fraction of the jet < 0.1
Type2	jet width	$W < 0.058$
Type2	JVT	JVT variable ≤ 0.56
Type2	BIB	use BIB tagging to remove fake jets from beam-halo muons
Type 0/1	no-CB	all muons of the LJ to be non-combined (“no-CB”)

Table 3: LJ signal selection requirements.

LJ - background estimation

- In order to extract the signal yield, taking into account the multijet and the cosmic-ray background residual contaminations, a data-driven likelihood-based ABCD method is used. This is a simultaneous data-driven background estimation and signal hypothesis test in the signal and control regions, robust against control regions with small number of events.

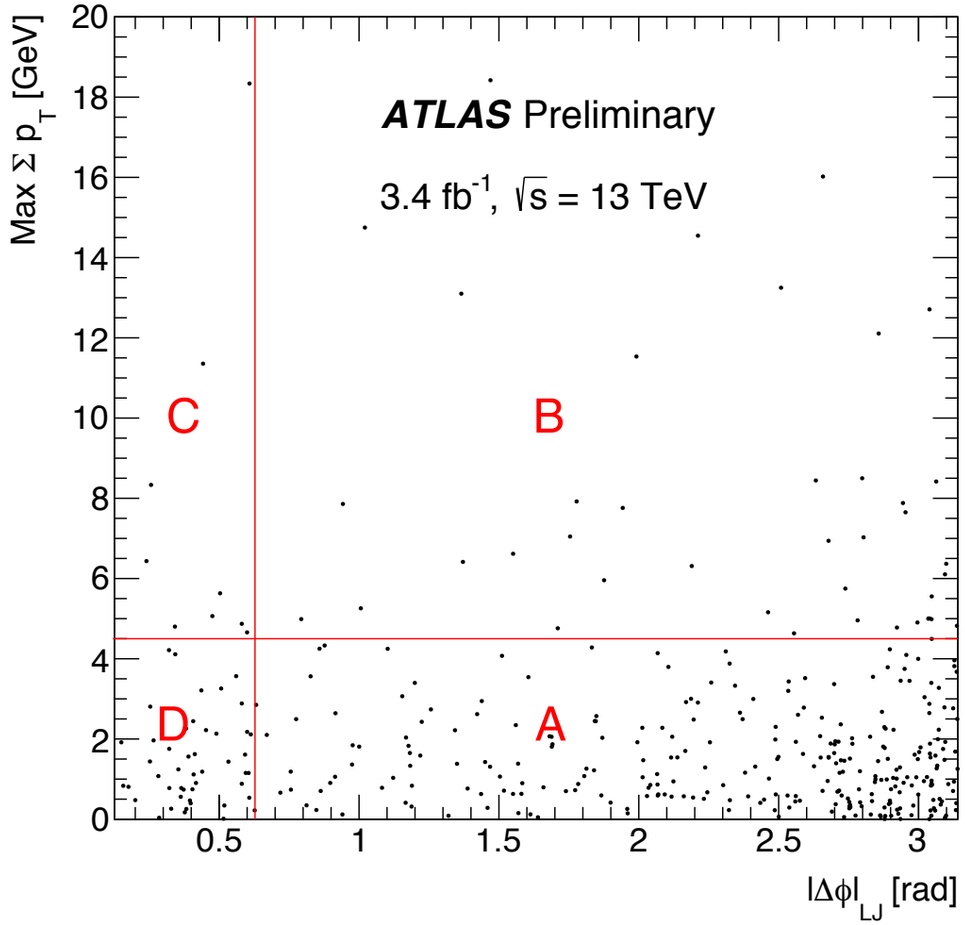

Limits

In the absence of a signal, the results of the search for LJ production with the likelihood-based ABCD method are used to set upper limits on the product of cross section and Higgs decay branching fraction to LJs, as a function of the γ_{d} mean lifetime, in the FRVZ models. Taking into account the relatively low signal efficiency for the Type2–Type2 event in all models and the high background, the Type2–Type2 events are excluded from the limit setting. The *CLs* method [58] is used to determine these limits, where the signal region is populated from the data-driven background estimate and from the appropriate signal hypothesis.

In order to determine these limits as a function of the γ_{d} lifetime the following procedure is used. The acceptance times efficiency with the selection criteria described above for the γ_{d} is evaluated as a function of the decay position L_{xy} (barrel) or L_{z} (endcap) and as a function of the p_{T} of the γ_{d} in the MC simulated FRVZ samples with lifetime $\mathrm{c}\tau = 47$ mm. A large number of MC pseudo experiments with different $\mathrm{c}\tau$ (ranging from 0.5 to 5000 mm) for the Higgs $\rightarrow 2\gamma_{\mathrm{d}} + X$ model are produced. For each γ_{d} of the pseudo experiments, the p_{T} and the η are extracted from the signal MC events at truth level, and the decay length from an exponential distribution with the proper decay length $\mathrm{c}\tau$ of the pseudo experiment; in this way the γ_{d} decay point in the detector is obtained. Using a matrix (constructed using the signal MC) describing the efficiency for reconstructing a γ_{d} of a given p_{T} and $\mathrm{c}\tau$, each event is weighted by the detection probability of its dark photons. The number of selected events in each pseudo experiment are then rescaled by the ratio of the integrated detection efficiency at a given $\mathrm{c}\tau$, $\varepsilon(c\tau)$, to the efficiency for the reference sample, $\varepsilon(47\text{ mm})$. This procedure is repeated separately for the Higgs $\rightarrow 4\gamma_{\mathrm{d}} + X$ benchmark model. Figure 9 shows, for the Higgs $\rightarrow 2\gamma_{\mathrm{d}} + X$ model, the ratio $\varepsilon(\mathrm{c}\tau)/\varepsilon(47\text{ mm})$ as a function of $\mathrm{c}\tau$. The solid black diamonds in the Figure show the relative efficiency found using full simulation Monte Carlo samples with $\mathrm{c}\tau = 4.7$ mm, 20 mm, 47 mm, and 470 mm, indicating a good agreement with the pseudo experiment process.

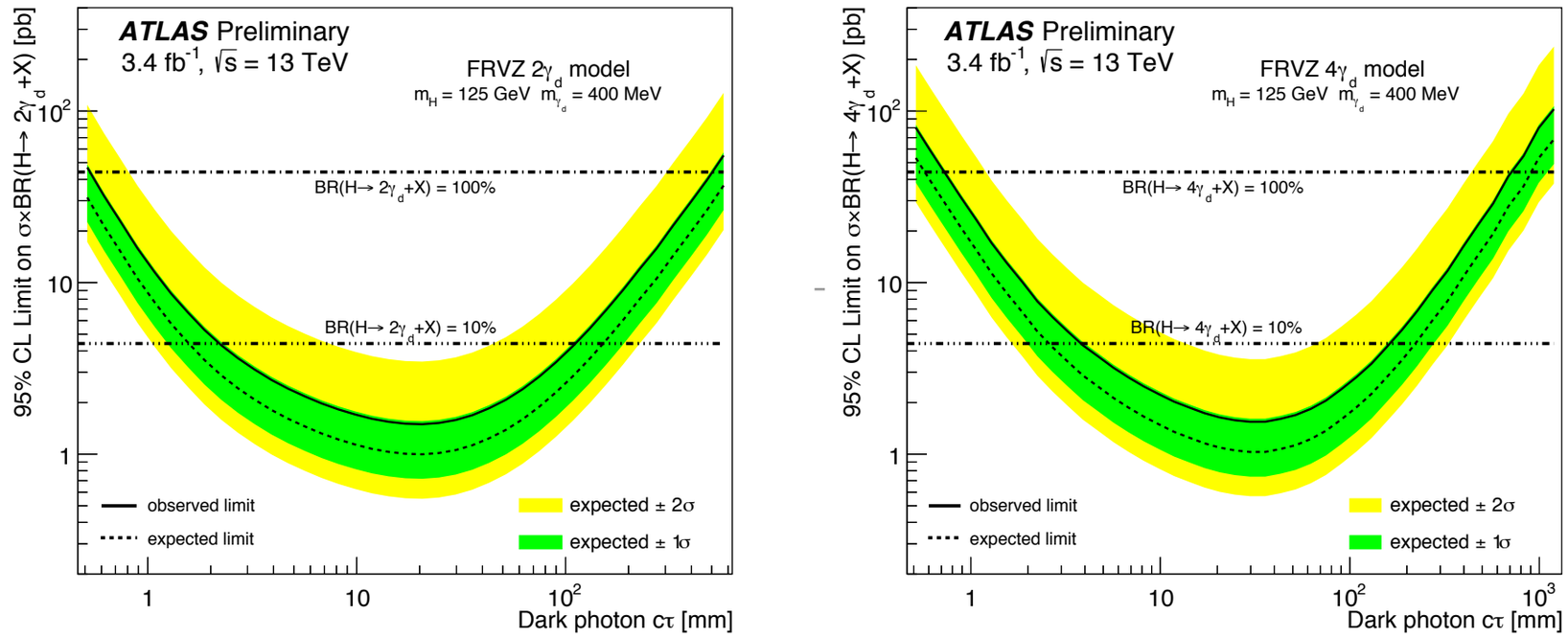

Figure 10: The 95% upper limits on the $\sigma\times$BR for the FRVZ 125 GeV Higgs $\rightarrow 2\gamma_{\mathrm{d}}+X$ (left) and Higgs $\rightarrow 4\gamma_{\mathrm{d}}+X$ (right) benchmark models as a function of the γ_{d} lifetime (cτ). The horizontal lines correspond to $\sigma\times$BR for two values of the BR of the Higgs boson decay to dark photons.

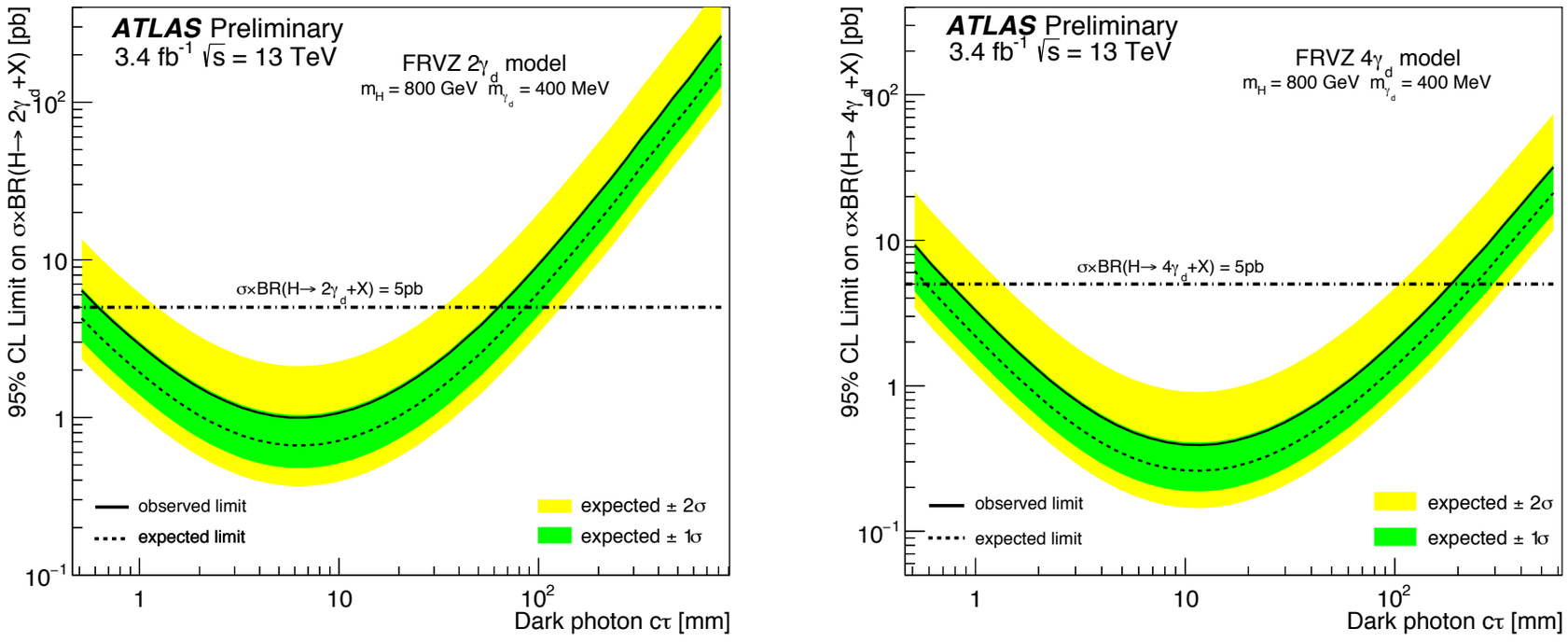

Figure 11: The 95% upper limits on the $\sigma\times$BR for the FRVZ 800 GeV Higgs $\rightarrow 2\gamma_{\mathrm{d}}+X$ benchmark model as a function of the γ_{d} lifetime (cτ). The horizontal lines correspond to a $\sigma\times$BR of 5 pb.

ATLAS

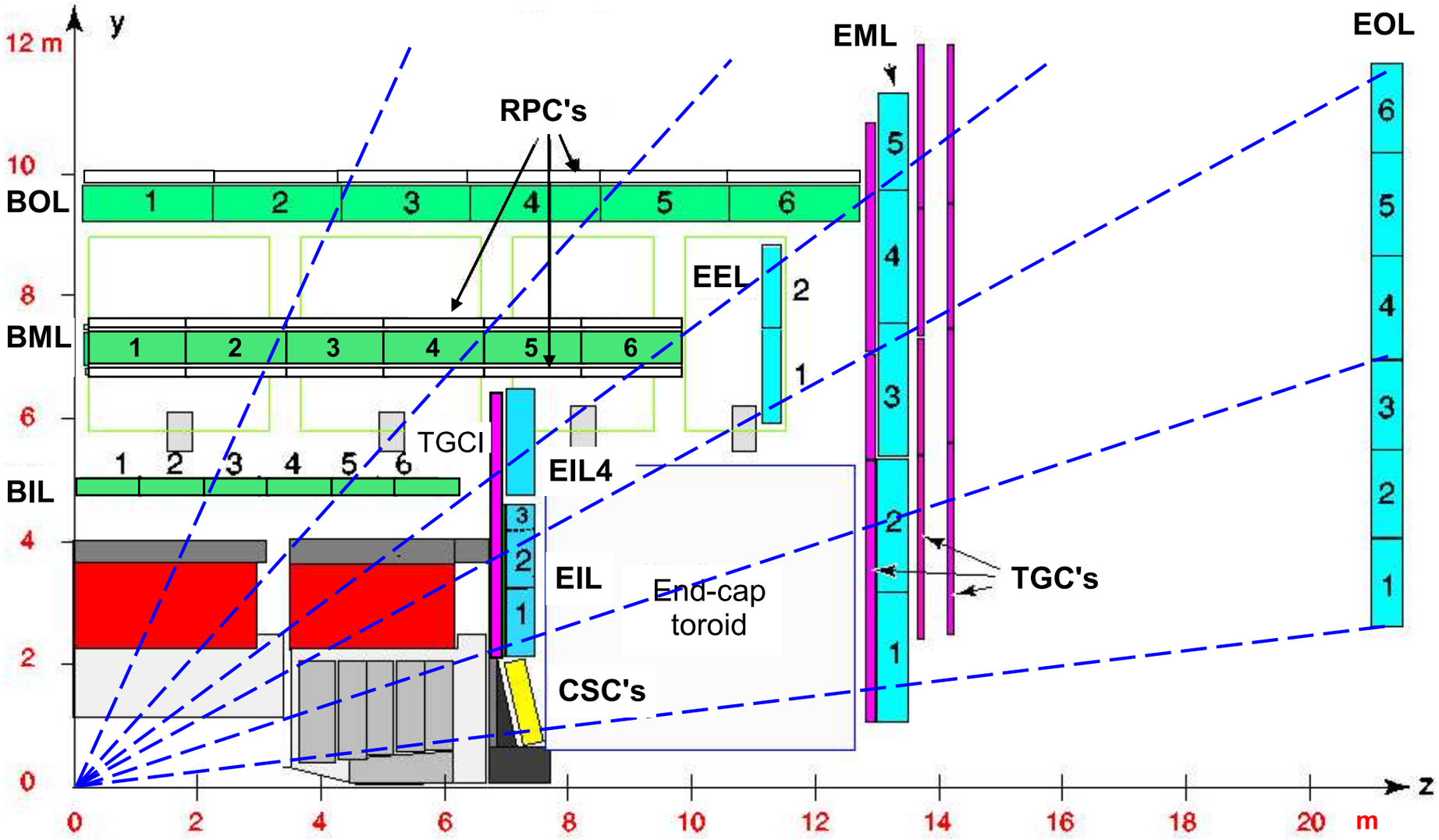
y
12 m
10
8
6
4
2
0
BOL
BML
BIL
1
2
3
4
5
6
RPC's
TGCI
EIL4
EIL
End-cap
toroid
CSC's
EML
EEL
TGC's
EOL
z
0
2
4
6
8
10
12
14
16
18
20
m